Carbohydrate Polymers 86 (2011) 513–519

Contents lists available at ScienceDirect

Carbohydrate Polymers

journal homepage: www.elsevier.com/locate/carbpol

Self-aggregates of cholesterol-modified carboxymethyl konjac glucomannan conjugate: Preparation, characterization, and preliminary assessment as a carrier of etoposide

Wei Ha [a], Hao Wu [a,c], Xiao-Ling Wang [c], Shu-Lin Peng [a], Li-Sheng Ding [a], Sheng Zhang [b,*], Bang-Jing Li [a,**]

[a] Key Laboratory of Mountain Ecological Restoration and Bioresource Utilization, Chengdu Institute of Biology, Chinese Academy of Sciences, Chengdu 610041, China
[b] State Key Laboratory of Polymer Materials Engineering, Polymer Research Institute of Sichuan University, Sichuan University, Chengdu 610065, China
[c] Ethenic Pharmaceutic Institute, Southwest University for Nationalities, Chengdu 610041, China

ARTICLE INFO

Article history:
Received 15 March 2011
Received in revised form 11 April 2011
Accepted 27 April 2011
Available online 11 May 2011

Keywords:
Carboxymethyl konjac glucomannan
Cholesterol
Nanoparticles
Drug carrier
Etoposide
In vitro release

ABSTRACT

Various cholesterol (CH) bearing carboxymethyl konjac glucomannan (CKGM) amphiphilic conjugates (denoted CHCKGM) were synthesized using CKGM as hydrophilic segments and CH as hydrophobic parts. Structural characteristics of these CHCKGM conjugates were investigated using FTIR, ^{1}H NMR and thermogravimetric analysis (TGA). The properties of these self-aggregates were analysed by dynamic laser light-scattering (DLS), zeta potential, transmission electron microscopy (TEM) and the fluorescence probe technologies. The critical aggregation concentration (cac) of CHCKGM conjugates (2.59×10^{-3} to 5.89×10^{-3} mg/mL) was comparatively low, suggesting that the cholesterol fragment was very effective for forming aggregates. Etoposide was physically entrapped into the CHCKGM nanoparticles by sonication method. The *in vitro* release behavior of etoposide from CHCKGM nanoparticles revealed a sustained release property. Furthermore, these self-aggregated nanoparticles showed pH- and ionic strength-dependent properties which caused a considerable change in their radius.

1. Introduction

Various polymeric amphiphiles have achieved increasing attention due to their special physicochemical and morphological properties in water (Gaucher et al., 2005; Kataoka, Harada, & Nagasaki, 2001; Nishikawa, Akiyoshi, & Sunamoto, 1996). Through non-covalent association arising from intra- and/or inter-molecular interactions among hydrophobic segments in the aqueous medium, these polymeric amphiphiles consisting of hydrophilic and hydrophobic segments can form micelle or micelle-like self-aggregates with hydrophobic cores and hydrophilic shells (Akiyoshi, 2002; Akiyoshi, Deguchi, Moriguchi, Yamaguchi, & Sunamoto, 1993; Dalhaimer, Bermudez, & Discher, 2004; Kakizawa, Harada, & Kataoka, 2001; Mortensen, 2001; Rotureau, Chassenieux, Dellacherie, & Durand, 2005;). Because these self-aggregates have potential uses in biotechnology and medicine fields due to their unique supramolecular structures, many polymeric amphiphiles have been explored, and their physicochemical properties also have been widely investigated (Benita & Levy, 1993; Jones & Leroux, 1999; Kang & Leroux, 2004; Qiu & Bae, 2007).

Konjac glucomannan (KGM), a high molecular weight and water soluble natural polysaccharide isolated from the tubers of the widespread plant *Amorphophallus konjac* in China and Japan, is composed of β-(1 → 4) linked β-D-glucose and β-D-mannose in the molar ratio 1:1.6–1:1.69 (Shimahara, Suzuki, Sugiyama, & Nishizawa, 1975). It is well-known that KGM has several advantages such as declining sugar level; promoting intestinal activity and weight loss; reducing the risk of diabetes and heart disease (Chen, Cheng, Liu, Liu, & Wu, 2006; Li, Xia, Wang, & Xie, 2005). Several chemical modification techniques have been applied to develop bio-related functional materials with better properties compared to the initial KGM (Du et al., 2004; Xia et al., 2010). CKGM is an anionic polymer obtained from the carboxymethylation of KGM. CKGM has been proven as a promising biomaterial in the drug delivery system due to its good water solubility, biocompatibility, bioactivity and excellent gelation ability when mixed with a polymer with opposite charge (Du et al., 2005a,b; Wang et al., 2008a). However, the synthesis and characterization of modified CKGM with hydropho-moieties and further using this amphiphile to form self-aggregated nanoparticles have not been reported yet.

Cholesterol is an indispensable structural building block in cells and plays a major role in many body functions. Cholesterol could be applied to modify some biomaterials due to highly hydrophobic sterol skeleton. It has been reported that cholesterol-bearing chitosan as a carrier showed stronger binding for hydrophobic guests' molecules and higher colloidal stability compared to

* Corresponding author. Tel.: +86 28 85400266; fax: +86 28 85402465.
** Corresponding author. Tel.: +86 28 85228831; fax: +86 28 85223843.
E-mail addresses: zslbj@163.com (S. Zhang), libj@cib.ac.cn (B.-J. Li).

0144-8617/$ – see front matter © 2011 Elsevier Ltd. All rights reserved.
doi:10.1016/j.carbpol.2011.04.083

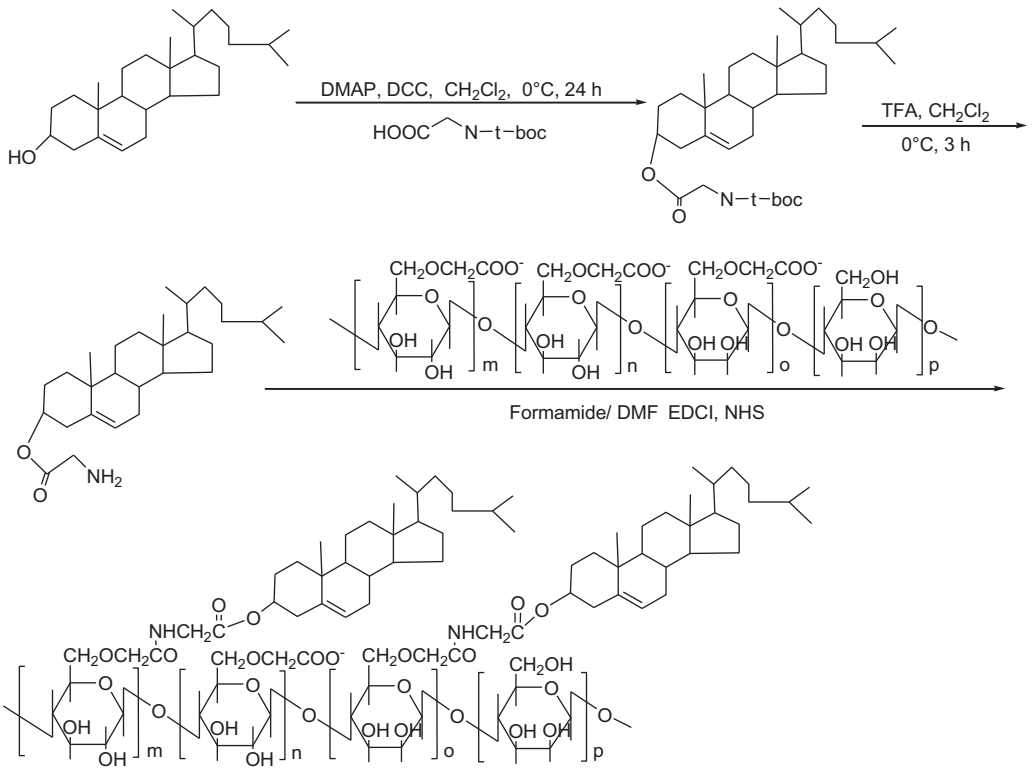

Scheme 1. Synthesis procedure of CHCKGM.

corresponding long alkyl chains (Akiyoshi, Yamaguchi, & Sunamoto, 1991). The cholesterol modified polymeric amphiphiles as carriers for hydrophobic drugs or genes have been developed extensively (Furgeson, Chan, Yockman, & Kim, 2003; Wang, Liu, Jiang, & Zhang, 2007a,b; Wang et al., 2008b; Yu, Li, Qiu, & Jin, 2008; Yuan, Li, & Yuan, 2006).

In this study, we designed and synthesized a novel self-assembled cholesterol-modified carboxymethyl konjac glucomannan (CHCKGM) conjugate via introducing cholesterol moieties (Scheme 1) into the glucose units of CKGM. By varying the feed ratio of cholesterol, a series of CHCKGM conjugates were prepared with different grafting ratios. The physicochemical and morphologic characteristics of these CHCKGM aggregates were also investigated in details. Furthermore, etoposide was chosen as a model drug to assess the potential of CHCKGM self-aggregated nanoparticles as a drug delivery carrier. Etoposide is an important antineoplastic agent used against several types of tumors, including testicular and small cell lung cancers, lymphoma, leukemia, and Kaposi's sarcoma (Issell, Rudolph, & Louie, 1984). However, etoposide has weak water solubility, etoposide therapy may cause some serious side effects such as low white blood counts, low platelet count, anemia, hair loss, soreness of the mouth and difficulty swallowing diarrhea (Falkson et al., 1975). Hence, it was expected that CHCKGM self-aggregated nanoparticles being used as a carrier for etoposide to improve its water solubility, sustain its release and give useful information for reducing the side effects of etoposide therapy.

2. Experimental methods

2.1. Materials and instrument

KGM was purchased from Chengdu Root Industry Co., Ltd. (Chengdu, China). Cholesterol, N-*tert*-butoxycarbonylglycine (N-*t*-Boc-glycine), 4-(dimethylamino) pyridine (DMAP), 1-ethyl-3-[3-(dimethylamino)propyl]-carbodiamide (EDC), dicyclohexylcarbodiimide (DCC), morpholinoethane sulfonic acid (MES), N-hydroxysuccinimide (NHS) and trifluoroacetic acid (TFA) were purchased from Sigma Aldrich (Shanghai, China).

All other reagents were of analytical grade and were used directly without further purification. All solvents and water were redistilled freshly.

CKGM was prepared as described by reference (Shimahara, Suzuki, Sugiyama, & Nishizawa, 1975). The degree of substitution was found to be 63.7% which measured according to methods described in the literature (Smith, 1967).

^{1}H NMRs were measured on a 600 MHz spectrometer (Avance Bruker-600, Switzerland). The chemical shifts of ^{1}H NMR are expressed in parts per million downfield relative to the internal tetramethylsilane (δ = 0 ppm) or chloroform (δ = 7.26 ppm). IR spectra were recorded on a Perkin Elmer spectrum one FT-IR spectrometer using KBr discs in the range of 400–4000 cm^{-1} region. The centrifugations were taken on TGL-20M, Saite Centrifuge Co., Shanghai, China. The absorbance value of the solution at 436 nm was recorded on APL-UV-2000 spectrophotometer, Shanghai, China. The dynamic light scattering (DLS) was measured by BI-9000AT, BI-200SM, Brookhaven Instruments Co., USA. The TEM were measured by Jeol JEM-100CX, and observation was done at an accelerating voltage of 80 kV. The fluorescence intensities were measured by Hitachi FP-7000, Japan. Zeta potential was measured by Malvern Nano ZSZEN 3600, England.

2.2. Synthesis of cholesterol glycinate (CHG)

Cholesterol (1 mmol) was dissolved into 10 mL anhydrous CH_2Cl_2 together with N-*t*-Boc-glycine (1.1 mmol) and DMAP (0.25 mmol). Subsequently, the reaction mixture was stirred at 0 °C for 24 h after the addition of 1.1 mmol of DCC. The dicyclohexylurea (DCU) was filtered off and then filtrate was concentrated in a vac-

uum at room temperature. The resultant was dissolved in a minimal amount of acetone and cooled overnight, and the precipitated DCU was filtered off. For the removal of *t*-boc group, cholesterol-*t*-boc-amino acid ester was dissolved in a mixture of CH_2Cl_2/TFA (1/1, v/v). The reaction mixture was stirred at 0 °C for 3 h and then evaporated to dryness. The deprotected derivative was dispersed in a 15% NaCl solution, and the pH was adjusted to 5.0. The solution was filtered to remove water insoluble *tert*-butyl salts. The filtrate was extracted three times with chloroform, the organic phases were combined and dried over Na_2SO_4. The Na_2SO_4 solid was filtered, and the solvent was evaporated. The obtained oily residue was finally dried under vacuum at room temperature.

IR (KBr, cm^{-1}): 3434 (NH_2-stretch), 2938 (C–H stretch), 1750 (C=O stretch), 1676 (NH_2 bending vibration), 1264 (C–N stretch), 1179 (C–O–C stretch).

^{1}H NMR ($CDCl_3$, ppm): 0.68 (3H, s, cholesterol 18-H_3), 0.9–2.4 (28H, cholesterol l-H_2, 2-H_2, 4-H_2, 7-H_2, 8-H_1, 9-H_1, 11-H_2, 12-H_2, 14-H_1, 15-H_2, 16-H_2, 17-H_1, 20-H_1, 22-H_2, 23-H_2, 24-H_2 and 25-H_1), 0.88 (6H, d J = 6.4 Hz, cholesterol 26-H_3 and 27-H_3), 0.93 (3H, dd, J = 6.24 Hz, 2.3 Hz, cholesterol 21-H_3), 1.01 (3H, s, cholesterol 19-H_3), 3.98 (2H, m, OCOCH_2–NH_2), 4.65 (lH, m, cholesterol 3-H_1), 5.37 (lH, m, cholesterol 6-H_1).

2.3. Synthesis of CHCKGM

A 0.5 mmol CKGM was dissolved in 10 mL formamide solution by water bath at 80 °C, then different amounts of EDC and NHS were mixed with CKGM solution at room temperature (the molar ratio of EDC:NHS:COO^- was 1:0.5:1), followed by addition of the DMF solution (10 mL) with different amounts of CHG. The resulting solution was stirred at room temperature under a nitrogen atmosphere for 24 h. After reaction, the mixture was precipitated in excessive acetone. The precipitate was carefully washed with water and THF to remove excessive CHG and CKGM. The precipitate was dispersed by water and dialysed by bag filter (MWCO: 8000–14000) at 25 °C for 72 h, and the solvent was lyophilized to obtain white powder.

IR (KBr, cm^{-1}): 3411 (OH-stretch), 2936 (C–H stretch), 1746 (C=O stretch), 1674 (amide stretch).

^{1}H NMR (DMSO, ppm): 0.67 (3H, s, cholesterol 18-H_3), 0.8–2.4 (28H, cholesterol l-H_2, 2-H_2, 4-H_2, 7-H_2, 8-H_1, 9-H_1, 11-H_2, 12-H_2, 14-H_1, 15-H_2, 16-H_2, 17-H_1, 20-H_1, 22-H_2, 23-H_2, 24-H_2 and 25-H_1), 0.88 (6H, dd J = 6.4 Hz, 2.3 Hz, cholesterol 26-H_3 and 27-H_3), 0.93 (3H, d, J = 6.24 Hz, cholesterol 21-H_3), 1.01 (3H, s, cholesterol 19-H_3), 3.0–4.5 (m, glucose and mannose ring 2, 3, 4, 5, 6-H_1), 3.98 (2H, m, OCOCH_2–NH_2), 4.63 (lH, m, cholesterol 3-H_1), 5.37 (lH, m, cholesterol 6-H_1).

2.4. Preparation of self-aggregated CHCKGM nanoparticles

CHCKGM self-aggregated nanoparticles were prepared by sonication in aqueous medium. Briefly, CHCKGM was dispersed in water under gentle shaking at room temperature for 24 h, followed by sonication for 2 min. To prevent heat build-up during the sonication, the pulse function was pulse on 2.0 s and pulse off 2.0 s. The sample solution was centrifuged at 7000 rpm to remove dust and impurity.

2.5. Self-aggregation behavior of CHCKGM conjugates

The CHCKGM conjugates suspension was prepared in the same way as the aggregate preparation. The aggregate solution was adjusted to various CHCKGM conjugate concentration, a known amount of pyrene in methanol was evaporated at 40 °C. A total of 3 mL of various concentration of sample suspension was added to each vial, and heated for 3 h at 65 °C to equilibrate the pyrene and the nanoparticles, and remained undisturbed to cool overnight at room temperature. The final concentration of pyrene was 1.0×10^{-6} M. Fluorescent spectra were measured using fluorescence spectrophotometer with a slit width of 10.0 and 2.5 nm for excitation and emission. For fluorescence emission spectra, excitation wavelength was set at 339 nm, and for fluorescence excitation spectra, the emission wavelength was set at 390 nm.

2.6. Particle size distribution and zeta potential

The sizes and size distributions of CHCKGM self-aggregated nanoparticles in water were determined using dynamic laser light-scattering (DLS) with a digital auto correlator at a scattering angle of 90°, a wavelength of 533 nm and a temperature of 25 °C. To investigate the relationship between the conjugates with different feed ratio of CHG and the size of nanoparticle, a series of CHCKGM self-aggregated nanoparticles in water with different feed ratio of CHG were prepared. Furthermore, in order to confirm whether the size of the CHCKGM self-aggregated nanoparticles could be affected by the pH and the ionic strength, a series of samples with different pH and concentrations of NaCl were prepared. The zeta potentials of CHCKGM self-aggregated nanoparticles in water were also measured.

2.7. Transmission electron microscopy (TEM)

To observe the morphology of CHCKGM self-aggregated nanoparticles, sample solutions (0.5 mg/mL) were dropped onto the carbon-coated 300 mesh copper grids. Then, the grids were air-dried and imaged using a transmission electron microscope.

2.8. Preparation of etoposide-loaded nanoparticles

4 mg CHCKGM and 1 mg etoposide was dispersed in water under gentle shaking at room temperature for 24 h, followed by sonication for 2 min. To prevent heat build-up during the sonication, the pulse function was pulse on 2.0 s and pulse off 2.0 s. The sample solution was centrifuged at 15,000 rpm to obtain etoposide loaded CHCKGM nanoparticles, and the nanoparticles were washed with deionized water three times to remove the etoposide, which was not entrapped inside the CHCKGM nanoparticles. The amount of etoposide was detected by UV spectrometry at 294 nm and calculated with standard curve plotted by the ΔA_{294nm} of the standard versus the etoposide concentration (the standard curve was plotted using a standard etoposide solution (Fig. S1). The etoposide encapsulation efficiency was calculated with the following equation:

$$\text{Encapsulation efficiency (\%)} = \frac{\text{mass of etoposide used in encapsulation} - \text{mass of free etoposide}}{\text{mass of etoposide used in encapsulation}} \times 100$$

2.9. In vitro release studies

Release rate measurements *in vitro* were carried out as follows: 2 mL etoposide loaded nanoparticles solution was placed in a dialysis bag (MWCO = 7000) and dialyzed against 10 mL of PBS. The release medium was stirred at 100 rpm at 30 °C. At predetermined sampling times; 4 mL medium was removed and replaced by 4 mL fresh PBS to maintain submersed conditions. The amount of etoposide in the solution was determined by UV spectrometry at 294 nm and calculated with the standard curve plotted by the ΔA_{294nm} of the standard versus the etoposide concentration (the standard curve was plotted using a standard etoposide solution, see Fig. S1).

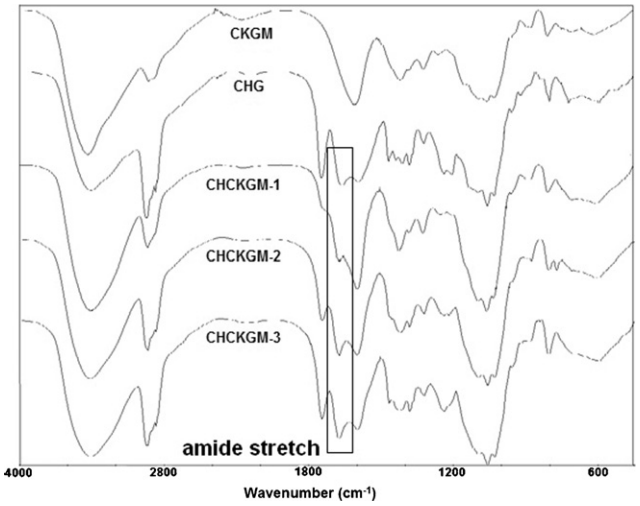

Fig. 1. FT-IR spectra of CHCKGM conjugates, CKGM and CHG.

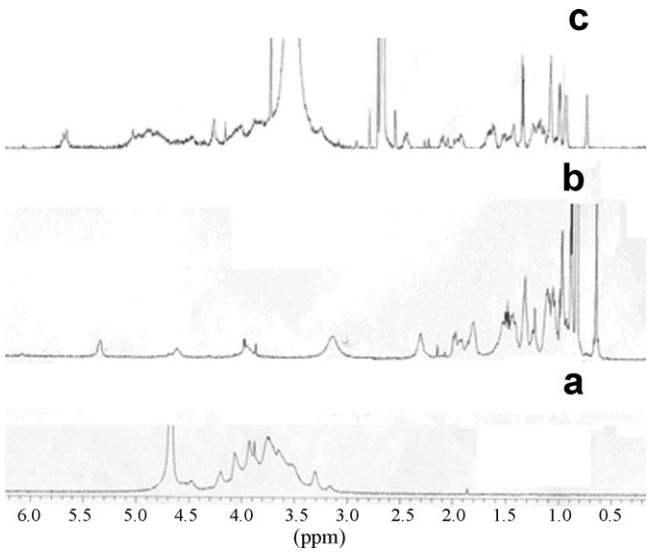

Fig. 2. ^{1}H NMR spectra for (a) CKGM in D_2O, (b) CHG in $CDCl_3$ and (c) CHCKGM-1 in DMSO.

3. Results and discussion

3.1. Preparation of CHCKGM conjugates

Scheme 1 shows the synthesis procedure of CHCKGM conjugates. An amino group was initially introduced to the cholesterol molecule using N-*tert*-butoxycarbonyl glycine by a two-step reaction. The CKGM was then coupled with the primary amino groups of cholesterols with "zero length" crosslinker of EDC/NHS afforded the final product CHCKGM.

Fig. 1 shows the IR spectra of CKGM and CHCKGMs with increasing feed ratio of CHG. The spectra of CKGM (Fig. 1a) show the following selected peaks: 3435 (O–H stretch), 2923 (C–H stretch), 1602 (C=O stretch of carboxyl methyl), 1059 (C–O–C stretch) (cm^{-1}). In Fig. 1b, the following selected IR peaks for CHCKGMs are shown: 3434 (OH stretch), 2938 (C–H stretch), 1750 (C=O stretch of ester bond), 1675 (NH_2 bending vibration), 1139–1264 (C–N stretch) (cm^{-1}). With increasing feed ration of CHG, the IR peaks of CHCKGMs in the region of 1668–1674 cm^{-1} (amide stretch) increased significantly, which confirmed the formation of an amide linkage between the primary amines of cholesterol and the carboxylates of CKGM. It can be seen that the intensity of amide stretch (1668–1674 cm^{-1}) is increasing with the feed ratios of cholesterol–glycine increased, which indicates the DS is increasing.

The ^{1}H NMR spectra of CKGM, CHCKGM and CHG are shown in Fig. 2, the proton assignment of CHG and CHCKGM are listed in experimental section. Compared with the proton signals of CKGM (Fig. 2a) and CHG (Fig. 2b), the more intensive $-CH_3$ peaks (δ 0.5–1.0) and double bond signal (δ 5.3) of CHG confirm the presence of cholesterol moieties (Fig. 2c). The characteristic peaks of CKGM appear between 3.0 and 4.8 ppm.

The TGA thermograms of CKGM, CHG and CHCKGM conjugates are shown in Fig. 3. The curves show that both CKGM and CHG involve two steps weight losses. The first slight weight loss at low temperatures can be attributed to the dryness procedure during heating and the subsequent second major weight loss can be attributed to the decomposition of CKGM (277 °C) or CHG (310 °C). In the cases of CHCKGM conjugates, three main stages of degradation could be observed: a moisture loss at a temperature around 100 °C, followed by a major weight loss of the CKGM component at about 270 °C and another subsequent weight loss of the CHG component around 300 °C. However, the weight loss of both CKGM and CHG component overlapped to one major weight loss stage because the decomposition temperature of CKGM and CHG is similar. The decomposition temperatures of the CHCKGM conjugates are higher than those of the pure CKGM indicating the enhanced thermal stability of CHCKGM conjugates.

3.2. Self-aggregation behavior of CHCKGM conjugates

The fluorescence probe technique was applied to study the self-aggregation behavior of CHCKGM conjugates on a molecular level. Pyrene was chosen as the fluorescent probe due its photophysical properties (Wilhelm et al., 1991). In a polar environment (water), pyrene shows only small fluorescence intensity due to its poor solubility and self-quenching, however, once the hydrophobic micro-domains in an aqueous solution was formed, pyrene will emits extensive radiation because its preferential locating inside or close to the hydrophobic micro-domains of micells. Therefore, pyrene is commonly used as a fluorescence probe to monitor the self-aggregation behavior of surfactants and/or polymers.

In low concentration range of CHCKGM conjugates, as shown in Fig. S2, the fluorescence excitation spectra of pyrene incorporated into various concentrations of CHCKGM self-assembled nanoparticles shows no significant change in the total fluorescence intensity. With the concentration increasing, however, the fluorescence intensity increased remarkably, reflecting the partitioning of pyrene into the hydrophobic microdomains of self-aggregates. The partitioning of pyrene led to the shift of the main peak, (0, 0) band, from 332 to 337 nm.

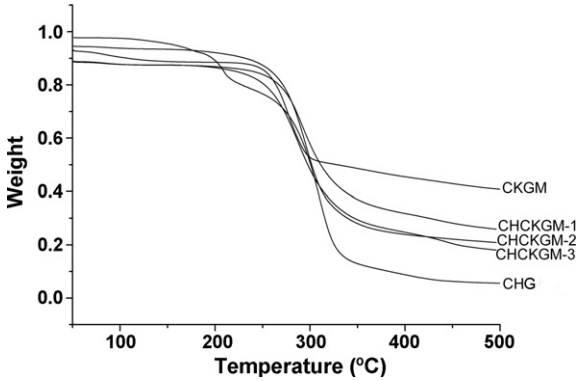

Fig. 3. TGA thermograms of CKGM, CHCKGMs and CHG.

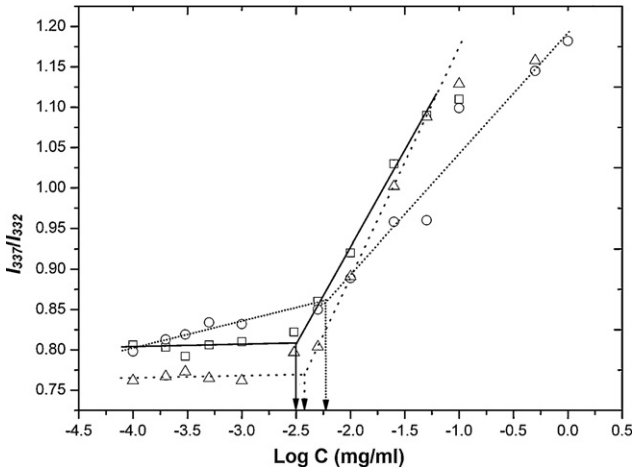

Fig. 4. Plot of the intensity ratio I_{337}/I_{332} (from pyrene excitation spectra) as a function of log C (CHCKGM-1, cycles; CHCKGM-2, triangles; CHCKGM-3, squares).

Fig. 4 demonstrates the intensity ratio (I_{337}/I_{332}) of the pyrene excitation spectra versus the logarithm of the concentration of CHCKGM. Critical aggregation concentration (cac), the threshold concentration of self-aggregate formation by intra- or intermolecular association, was determined from the crossover point in the low concentration ranges. The cac values (Table 1) of the CHCKGM conjugates are in the range of 2.59×10^{-3} to 5.89×10^{-3} mg/mL, which are one order of magnitude lower than those of low molecular weight surfactants (Nagasaki et al., 1998), and even more lower than those of other polymeric amphiphiles (Kim et al., 2000; Kim, Lee, Kwon, Chung, & Jeong, 2002), including other cholesterol-modified aggregates (Wang, Liu, Jiang, & Zhang, 2007a; Yu, Li, Qiu, & Jin, 2008). The higher feed ratio of the cholesterol moiety induces the lower cac. The low cac value implies that the self-aggregates can be formed easily by modified CKGM and the corresponding aggregates maintain the stability in dilute condition. The major driving force for the aggregation of amphiphiles is ascribed to the hydrophobic interaction between hydrophobic moieties. It seemed that the cholesterol segments offered strong binding sites and was very efficient for the formation of aggregates. Therefore, the cholesterol modified CKGM conjugates are the promising alternatives to encapsulate substances via hydrophobic interaction.

3.3. Preparation and characterization of CHCKGM self-aggregated nanoparticles

Self-aggregated nanoparticles were formed by sonication when CHCKGM conjugates were dispersed in water at the concentration of 0.5 mg/mL. Increasing the feed ratio of cholesterol moiety results in the smaller size of the nanoparticles (Table 1), although there is tiny difference in CHCKGM-2 and CHGKGM-3. These results suggest that the higher grafting density of the hydrophobic cholesterol grafts favor to smaller aggregates. This trend of the size variation with graft density is consistent with the micells of graft copolymers in selective solvent (Hu et al., 2008).

The morphology of self-aggregates was investigated by TEM (Fig. 5). As shown in Fig. 5a–c, those nanoparticles are almost sphere. From the TEM images, the size of these nanoparticles decreased from 400 nm to less than 100 nm with feed ratio of cholesterol moiety increasing from 0.3 to 1. However, as shown in Table 1, the sizes of the self-aggregated nanoparticles measured by DLS are in the range from 1033 to 391 nm, which were obviously larger than the sizes determined by TEM. We believe this may result from the shrinkage of particles during the process of the solvent evaporation in the samples preparation.

As shown in Fig. 5d, the zeta potential of CHCKGM-1 self-aggregated nanoparticles in water were negative, and the absolute value of zeta potential of CHCKGM-1 self-aggregated nanoparticles was 30.8 ± 1 mV, suggesting that the negative charged carboxymethyl group in CKGM molecules were mainly distributed on the surface of self-aggregated nanoparticles due to their hydrophilic property.

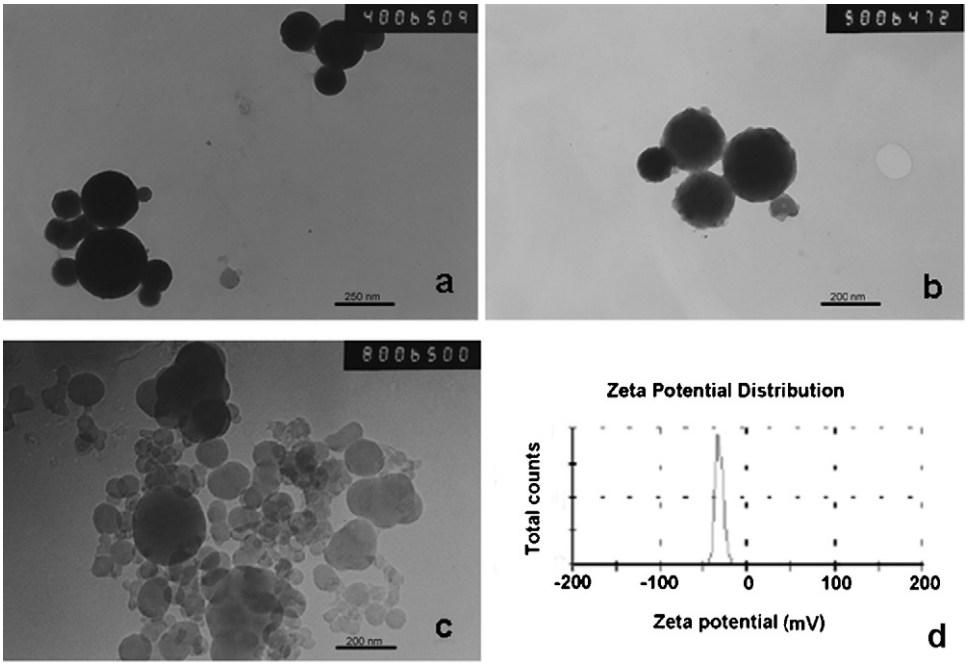

Fig. 5. (a) TEM image of CHCKGM-1, (b) TEM image of CHCKGM-2, (c) TEM image of CHCKGM-3, (d) zeta potential of CHCKGM-1.

Table 1
Characterization of CHCKGM self-aggregated nanoparticles.

Samples[a]	Feed mole ratio[b]	CAC × 10^{-3} (mg/mL)	Diameter (nm)	Polydispersity index
CHCKGM-1	0.3:1	5.89	1033 ± 47	0.223 ± 0.047
CHCKGM-2	0.5:1	3.89	477 ± 30	0.126 ± 0.027
CHCKGM-3	1:1	2.59	391 ± 23	0.246 ± 0.002

[a] CHCKGM conjugates, where the number indicates the increasing feed ratio of CH.
[b] Mole ratio of CH: the sugar units of CKGM.

3.4. Drug loading and in vitro drug release study

Etoposide was the first agent recognised as a topoisomerase II inhibiting anticancer drug. Research on etoposide helps the understanding of mechanisms by which the drugs poison topoisomerase II. With the demonstrated antineoplastic activity of the drug, FDA approval was granted for etoposide in 1983. Up to now, the work to improve the therapeutic index of etoposide mostly focused on dose-regimens and pharmaceutical preparation (Hande, 1998). Therefore, we developed a new method by using a carrier for loading etoposide, which aimed at improving its therapeutic index.

The incorporation of etoposide into the CHCKGM-2 particles occurred simultaneously during sonication and the encapsulation efficiency achieved to 39.4%. The *in vitro* release profile of etoposide from etoposide/CHCKGM-2 particles was presented in Fig. 6. The etoposide appeared to be released in a biphasic way, which characterized by an initial rapid release period followed by a step of slower release. The burst effect was observed in 2 h, in which 55% of the drug was released from the nanoparticles. After this initial effect, etoposide was released in a continuous way for up to 23 h, reaching to close 96% of cumulative release.

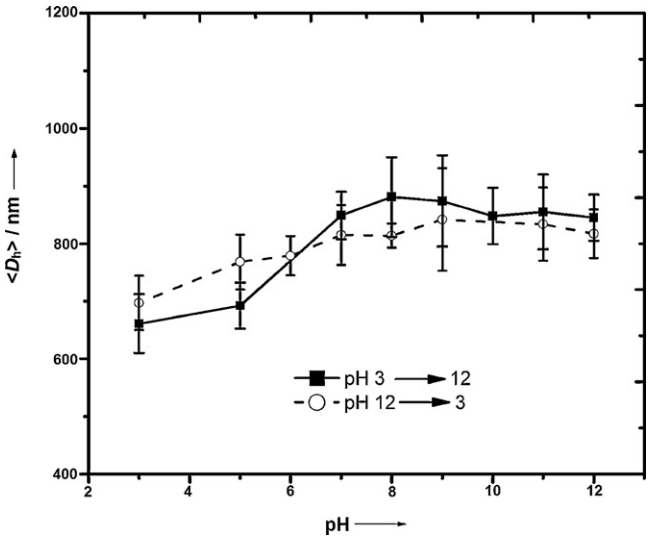

Fig. 7. Average hydrodynamic diameter $\langle D_h \rangle$ of CHCKGM-1 self-aggregated spheres as a function of pH.

3.5. pH and ionic strength effects on CHCKGM nanoparticles

The conformation of polyelectrolytes is very sensitive towards the physicochemical conditions of their surrounding medium (e.g., ionic strength, pH, or presence of multivalent ions). With the pH increasing, the carboxyl groups of the CKGM segment are progressively neutralized corresponding to more hydrophilic $-COO^-$ groups formation. As a result of the associated electrostatic repulsion between the increasing numbers of identically charged carboxylate anions along the CKGM backbone, the shells of such particles should swell considerably upon increasing the pH. As shown in Fig. 7, the particles radius increases from 660 nm to 880 nm as the pH increases from 4 to 8. When the environmental pH is adjusted to 8 or higher, the radius of the particles tends towards to a saturation value. It is worth noting that this change is completely reversible. When the pH is adjusted from 12 to 3, similar results have also been observed. The extension of this expansion depends on ionic strength of the aqueous solution at given pH value. The effect of varying salt (NaCl) concentration is shown in Fig. 8, as can directly be seen that the swelling of the particles increases with increasing salt concentration due to more intense electrostatic shielding effects. Similar observations have been made with other polyelectrolytes based particles (Liu & Armes, 2003).

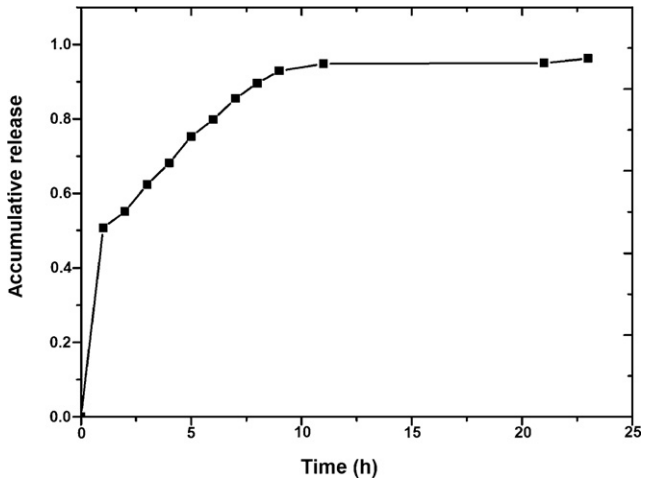

Fig. 6. Etoposide release from etoposide/CHCKGM-2 nanoparticles at 30 °C in PBS (pH 7.4).

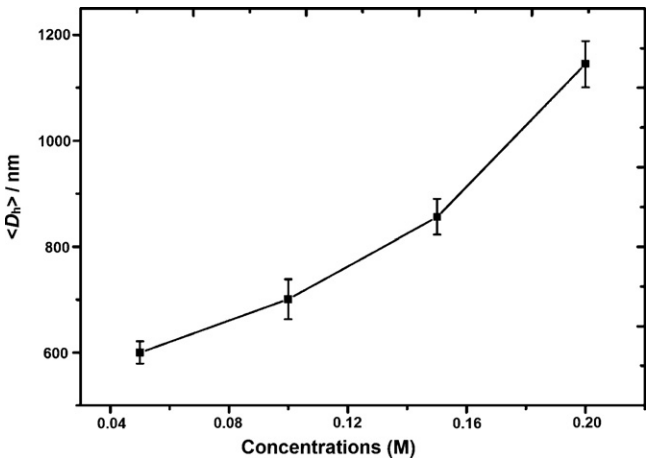

Fig. 8. Average hydrodynamic diameter $\langle D_h \rangle$ of CHCKGM-1 self-aggregated spheres as a function of NaCl concentrations.

4. Conclusion

In summary, novel carboxymethyl konjac glucomannan conjugates with cholesterol conjugates were synthesized and characterised. These polymeric amphiphiles can form self-aggregates in aqueous media. The cac values of conjugates are smaller than 5.89×10^{-3} mg/mL, indicating that the cholesterol residue is very effective to form aggregates. Those self-aggregates exhibit a pH- and ionic strength-dependent properties causing a considerable increase (decrease) of their radius. Hydrophobic drug etoposide was successfully entrapped into the CHCKGM nanoparticles and its release behavior *in vitro* exhibited a sustained release. These preliminary results indicated that CHCKGM self-aggregates could be a potential drug carrier for the drug delivery.

Acknowledgements

This project is supported by National Natural Science Foundation of China (NSFC Grant Nos. 21074138, 51073107 and 50703025), CAS Innovation Program (Grant No. KSCX2-EW-J-22) and the Opening Project of State Key Laboratory of Polymer Materials Engineering (Sichuan University) (KF201003).

Appendix A. Supplementary data

Supplementary data associated with this article can be found, in the online version, at doi:10.1016/j.carbpol.2011.04.083.

References

Akiyoshi, K. (2002). *Supramolecular design for biological applications*. Boca Raton: CRC Press., pp. 13–24

Akiyoshi, K., Yamaguchi, S., & Sunamoto, J. (1991). Self-aggregates of hydrophobic polysaccharide derivatives. *Chemistry Letters*, *20*, 1263–1266.

Akiyoshi, K., Deguchi, S., Moriguchi, N., Yamaguchi, S., & Sunamoto, J. (1993). Self-aggregates of hydrophobized polysaccharides in water. Formation and characteristics of nanoparticles. *Macromolecules*, *26*, 3062–3068.

Benita, S., & Levy, M. Y. (1993). Submicron emulsions as colloidal drug carriers for intravenous administration: Comprehensive physicochemical characterization. *Journal of Pharmaceutical Sciences*, *82*, 1069–1079.

Chen, H. L., Cheng, H. C., Liu, Y. J., Liu, S. Y., & Wu, W. T. (2006). Konjac acts as a natural laxative by increasing stool bulk and improving colonic ecology in healthy adults. *Nutrition*, *22*, 1112–1119.

Dalhaimer, P., Bermudez, H., & Discher, D. E. (2004). Biopolymer mimicry with polymeric wormlike micelles: Molecular weight scaled flexibility, locked-in curvature, and coexisting microphases. *Journal of Polymer Science Part B: Polymer Physics*, *42*, 168–176.

Du, J, Sun, R., Zhang, S., Govender, T., Zhang, L. F., Xiong, C. D., et al. (2004). Novel polyelectrolyte carboxymethyl konjac glucomannan–chitosan nanoparticles for drug delivery. *Macromolecular Rapid Communications, 25*, 954–958.

Du, J., Sun, R., Zhang, S., Zhang, L. F., Xiong, C. D., & Peng, Y. X. (2005). Novel polyelectrolyte carboxymethyl konjac glucomannan–chitosan nanoparticles for drug delivery. I. Physicochemical characterization of the carboxymethyl konjac glucomannan–chitosan nanoparticles. *Biopolymers*, *78*, 1–8.

Du, J., Zhang, S., Sun, R., Zhang, L. F., Xiong, C. D., & Peng, Y. X. (2005). Novel polyelectrolyte carboxymethyl konjac glucomannan–chitosan nanoparticles for drug delivery. II. Release of albumin in vitro. *Journal of Biomedical Materials Research Part B: Applied Biomaterials*, *72B*, 299–304.

Falkson, G., Van Dyk, J. J., Van Eden, E. B., Van Der Merwe, A. M., Van Der Bergh, J. A., & Falkson, H. C. (1975). A clinical trial of the oral form of 4′-demethyl-epipodophyllotoxin-β-D-ethylidene glucoside (NSC 141540) VP 16-213. *Cancer*, *35*, 1141–1144.

Furgeson, D. Y., Chan, W. S., Yockman, J. W., & Kim, S. W. (2003). Modified linear polyethylenimine–cholesterol conjugates for DNA complexation. *Bioconjugate Chemistry*, *14*, 840–847.

Gaucher, G., Dufresne, M.-H., Sant, V. P., Kang, N., Maysinger, D., & Leroux, J.-C. (2005). Block copolymer micelles: Preparation, characterization and application in drug delivery. *Journal of Controlled Release*, *109*, 169–188.

Hande, K. R. (1998). Etoposide: Four decades of development of a topoisomerase II inhibitor. *European Journal of Cancer*, *34*, 1514–1521.

Hu, Y., He, X. R., Lei, L., Liang, S., Qiu, G. F., & Hu, X. M. (2008). Preparation and characterization of self-assembled nanoparticles of the novel carboxymethyl pachyman-deoxycholic acid conjugates. *Carbohydrate Polymers*, *74*, 220–227.

Issell, B. F., Rudolph, A. R., & Louie, A. C. (1984). *Etoposide (VP-16), current status and new developments*. New York: Academic Press., pp. 6–8.

Jones, M. C., & Leroux, J. C. (1999). Polymeric micelles – A new generation of colloidal drug carriers. *European Journal of Pharmaceutics and Biopharmaceutics*, *48*, 101–111.

Kakizawa, Y., Harada, A., & Kataoka, K. (2001). Glutathione-sensitive stabilization of block copolymer micelles composed of antisense DNA and thiolated poly(ethylene glycol)-block-poly(L-lysine): A potential carrier for systemic delivery of antisense DNA. *Biomacromolecules*, *2*, 491–497.

Kang, N., & Leroux, J. C. (2004). Triblock and star-block copolymers of N-(2-hydroxypropyl) methacrylamide or N-vinyl-2-pyrrolidone and D,L-lactide: Synthesis and self-assembling properties in water. *Polymer*, *45*, 8967–8980.

Kataoka, K., Harada, A., & Nagasaki, Y. (2001). Block copolymer micelles for drug delivery: Design, characterization and biological significance. *Advanced Drug Delivery Reviews*, *47*, 113–131.

Kim, C., Lee, S. C., Kang, S. W., Kwon, I. C., Kim, Y.-H., & Jeong, S. Y. (2000). Synthesis and the micellar characteristics of poly(ethylene oxide)-deoxycholic acid conjugates. *Langmuir*, *16*, 4792–4797.

Kim, C., Lee, S. C., Kwon, I. C., Chung, H., & Jeong, S. Y. (2002). Complexation of poly(2-ethyl-2-oxazoline)-block-poly(ε-caprolactone) micelles with multifunctional carboxylic acids. *Macromolecules*, *35*, 193–200.

Li, B., Xia, J., Wang, Y., & Xie, B. J. (2005). Grain-size effect on the structure and antiobesity activity of konjac flour. *Journal of Agricultural and Food Chemistry*, *53*, 7404–7407.

Liu, S. Y., & Armes, S. P. (2003). Synthesis and aqueous solution behavior of a pH-responsive schizophrenic diblock copolymer. *Langmuir*, *19*, 4432–4438.

Mortensen, K. (2001). Structural properties of self-assembled polymeric aggregates in aqueous solutions. *Polymers for Advanced Technologies*, *12*, 2–22.

Nagasaki, Y., Okada, T., Scholz, C., Iijima, M., Kato, M., & Kataoka, K. (1998). The reactive polymeric micelle based on an aldehyde-ended poly(ethylene glycol)/poly(lactide) block copolymer. *Macromolecules*, *31*, 1473–1479.

Nishikawa, T., Akiyoshi, K., & Sunamoto, J. (1996). Macromolecular complexation between bovine serum albumin and the self-assembled hydrogel nanoparticle of hydrophobized polysaccharides. *Journal of the American Chemical Society*, *118*, 6110–6115.

Qiu, L. Y., & Bae, Y. H. (2007). Self-assembled polyethylenimine-graft-poly(e-caprolactone) micelles as potential dual carriers of genes and anticancer drugs. *Biomaterials*, *28*, 4132–4142.

Rotureau, E., Chassenieux, C., Dellacherie, E., & Durand, A. (2005). Neutral polymeric surfactants derived from dextran: A study of their aqueous solution behavior. *Macromolecular Chemistry and Physics*, *206*, 2038–2046.

Shimahara, H., Suzuki, H., Sugiyama, N., & Nishizawa, K. (1975). Isolation and characterization of oligosaccharides from an enzymic hydrolysate of konjac glucomannan. *Agricultural Biology and Chemistry*, *39*, 293–299.

Smith, R. J. (1967). *Starch: Chemistry and technology*. New York: Academic Press., pp. 621–625.

Wang, Y. S., Liu, L. R., Jiang, Q., & Zhang, Q. Q. (2007). Self-aggregated nanoparticles of cholesterol-modified chitosan conjugate as a novel carrier of epirubicin. *European Polymer Journal*, *43*, 43–51.

Wang, Y. S., Liu, L. R., Weng, J., & Zhang, Q. Q. (2007). Preparation and characterization of self-aggregated nanoparticles of cholesterol-modified O-carboxymethyl chitosan conjugates. *Carbohydrate Polymers*, *69*, 597–606.

Wang, R., Xia, B., Li, B. J., Peng, S. L., Ding, L. S., & Zhang, S. (2008). Semi-permeable nanocapsules of konjac glucomannan–chitosan for enzyme immobilization. *International Journal of Pharmaceutics*, *364*, 102–107.

Wang, Y. S., Jiang, Q., Li, R. S., Liu, L. L., Wang, Y. M., Zhang, Q. Q., et al. (2008). Self-assembled nanoparticles of cholesterol-modified O-carboxymethyl chitosan as a novel carrier for paclitaxel. *Nanotechnology*, *19*, 145101.

Wilhelm, M., Zhao, C. L., Wang, Y. C., Xu, R. L., Winnik, M. A., Mura, J. L., et al. (1991). Poly(styrene-ethylene oxide) block copolymer micelle formation in water: A fluorescence probe study. *Macromolecules*, *24*, 1033–1040.

Xia, B., Ha, W., Meng, X. W., Govende, T., Peng, S. L., Ding, L. S., et al. (2010). Preparation and characterization of a poly(ethylene glycol) grafted carboxymethyl konjac glucomannan copolymer. *Carbohydrate Polymers*, *79*, 648–654.

Yu, J. M., Li, Y. J., Qiu, L. Y., & Jin, Y. (2008). Self-aggregated nanoparticles of cholesterol-modified glycol chitosan conjugate: Preparation, characterization, and preliminary assessment as a new drug delivery carrier. *European Polymer Journal*, *44*, 555–565.

Yuan, X. B., Li, H., & Yuan, Y. B. (2006). Preparation of cholesterol-modified chitosan self-aggregated nanoparticles for delivery of drugs to ocular surface. *Carbohydrate Polymers*, *65*, 337–345.